Journal of Materials and Environmental Science
ISSN : 2028-2508
CODEN : JMESCN

J. Mater. Environ. Sci., 2020, Volume 11, Issue 5, Page 723-735

http://www.jmaterenvironsci.com

Modified Hybrid Flame Retardant in Wood Sawdust-Polyester Particleboard: Characterization and Flame Retardancy

T.O. Suoware[1], C.O. Amgbari[1], B.N. Ugwu[2], I.O. Ofondu[2], E. Amula[3], F.K. Sorgbara[1] and I.J. Adukeh[1]

1. Department of Mechanical Engineering Technology, Federal Polytechnic, Ekowe, Nigeria
2. Department of Mechanical and Production Engineering, Enugu State University of Science and Technology, Nigeria
3. Department of Mechanical Engineering, Niger Delta University, WilberForce Island, Nigeria

Received 22 Oct 2019,
Revised 12 April 2020,
Accepted 13 April 2020

Keywords
- ✓ *Flame Retardant,*
- ✓ *Flammability properties,*
- ✓ *Flame spread,*
- ✓ *Particleboard,*
- ✓ Wood Sawdust,

suoware.research@gmail.com,
Phone: +2347037201960

Abstract
Ammonium polyphosphate (APP) was modified with Gum Arabic Powder (GAP) and combined with Aluminium hydroxide (ATH) and then synergized with carbon black (CB) to form hybrid flame retardant (FR) species. The FR species were incorporated in wood sawdust polyester particleboard (WSPP) during processing using hand lay compression moulding. The particleboard were characterized by impact tester, cone calorimeter at $50kWm^{-2}$ heat flux and radiant panel as well as the performance in real scale using existing predictive model. The hybridized synergistic specie modified by GAP to form $WSPP_{15\%APP-GAP/CB}$ particleboard did not only show an outstanding performance on flame retardancy but maintained same impact strength with those without FR ($WSPP_{0\%}$). Char residue show that GAP present in the FR specie achieved a stable and compact char structure which prevented the release of combustible volatiles and attained an improved peak heat release rate of $78kWm^{-2}$ compared to $WSPP_{0\%}$ at $195.5kWm^{-2}$. Radiant panel results show that the $WSPP_{15\%APP-GAP/CB}$ particleboard weakens the flame spread energy responsible for heat transfer better from 24.0 to $7.17kW^{2}s^{-3}$ due to the mechanism of APP-GAP during burning. Based on model predictions, the fire growth rate (FIGRA) in real scale fire scenario shows that the FR formulations could meet established fire safety standards for interior building applications according to Euro-class criteria.

1. Introduction
The use of wood residue having lignocellulosic properties bonded in either synthetic or biopolymer matrix to obtain composite particleboards for various industrial applications has grown in the last decades. Interior and exterior applications such as ceiling boards, wall partitions, window and doors, fencing and cladding etc. [1, 3] as well as non-structural automotive component parts [4] are some examples which have been successfully accomplished using particleboards. The increase in use is probably as a result of the significant advantages they possess which includes lightweight, low cost and maintenance, wood-like appearance, durability and stiffness [5-7]. Notwithstanding, sawdust like any other lignocellosic fibre or particle such as hemp, coir, bagasse, flax, kenaf, etc. reinforced in polymer matrix when exposed to heat, release combustible products that can combust and spread flame that are sometimes very destructive. This has restricted their use in areas where stringent fire regulations do not exist. For the particleboard to meet current fire safety standards, several researchers [8-12] have focused their attention to improve the flame retardancy of wood based polymer composites by traping combustible volatiles that can caue high release rates.

Flame retardant (FR) are chemical substances classified as either halogenated based FR (HBFR) or halogenated free FR (HFFR) that are incorporated into the fibre or particulate base composite during processing either by graft copolymerization [13] or intimately blended into the polymer using a high mechanical stirring device respectively. HBFR that is bromine or chlorine are effective for polymeric composites as they inhibit flame during a combustion process by ensuring that volatile gas mixtures when oxidized does not exceed the lower flammability limit. However, the consequences with HBFR are that they release smoke containing corrosive, acidic and toxic gases that are of serious health and environmental concerns [13-14]. Hence, the need for a greener, with low toxicity and environmentally friendly based FR. Aluminium hydroxide (ATH) is a low cost HFFR which is widely used in polymers, upon decomposition ATH releases water vapour which dilutes the combustible gases of the polymer and at the same time form aluminium oxide (Al_2O_3) which acts as a barrier to the mass transfer of heat. ATH generally serves threefold purpose as reported by Liang and Zhang [15] and Weng et al [16] which includes; filler, FR and smoke suppressant but the high loading up to 60% impacts negatively on mechanical properties as well as material cost. Ammonium polyphosphates (APP) is the most favourable HFFR for polymers, wood and wood based polymer composite [9, 17-24], due to its high efficiency and low toxicity. APP is said to promote intumescent char layer which acts as physical barrier to slow the mass transfer of heat.

The effect of the hybridized form of ATH and APP in polymer composite is not clearly understood. Wang *et al* [25] reports that the combined FRs could be influenced by a number of factors which includes; specific polymer system, ratio of ATH/APP, viscosity of the decomposition product and fire scenario. Kahlili *et al* [26] also reported in their work that ATH and APP alone exhibited much lower flame retardant behaviour, lower mass residue and higher gross heat of combustion than the hybridized system (ATH/APP). Besides, the low hydrolytic stability and low compatibility of APP with polymers impacts negatively on the durability and physical-mechanical properties of the composite. Also, the high moisture sensitivity with poor compatibility associated with APP intumescent FR formulation causes problems in achieving homogenous blend in polymer composites. Thus, from previous studies it shows that the improvement in the viscosity during decomposition and increase in mass residue of composites play a key role in preventing the collapse of foamed structure that is needed to improve the flammability behaviour of polymer composite. Therefore, the aim of this paper is to investigate the effect of incorporating Gum Arabic powder (GAP) in hybrid FR; ATH and APP which is novel and then synergised with carbon black (CB) to improve residual mass and thus better improve flame retardancy of the WSP particleboard as well as meet with established building fire standard using existing predictive model.

2. Material and Methods

2.1. Particleboard Materials

Wood sawdust used in fabricating the composite particleboard was sourced at sawmill dump site within the University of Nigeria, Nsukka community. Flame retardants consisting of aluminium hydroxide [Al_2O_3] of particle size 10µm, ammonium polyphosphate [NH_4PO_3]n a white-free flowing powder soluble in g/100ml of H_2O with average particle size of 15µm and carbon black[CB: purity>90%] of particle size 300µm, litmus paper, distilled water and the polyester resin used were supplied by Joe Chem ventures. Gum Arabic purchased in the Northern part of Nigeria was further processed into a fine powder of particle size 300 µm used as a binder and source of carbohydrate to formulate new flame retardant specie. Unsaturated polyester resin (UPR) was cured with 2% methyl ethyl ketone peroxide (MEKP) as catalyst and 1% cobalt (Co) as accelerator. All chemicals were used without further purification. Note that the exact chemical structure of UPR was note supplied by the manufacturer.

2.2 Fabrication FR-WSP Particleboard

Fine ground wood sawdust (WS) as shown in Figure 1a were first treated with 5% (NaOH) solution for about 2hrs as displayed in Figure 1b to improve the compatibility with the polyester resin (PR). Afterwards, the particulates were washed with distilled water until blue litmus paper turned red which indicates that excess concentration of NaOH have been neutralized and then oven dried for 3hrs to remove moisture content as shown in Figure 1c. The ready to use wood particles in Figure 1d were used to fabricate the particleboard using hand lay-up compression moulding technique as shown in Figure 1e. The required quantities of the sawdust and PR were used to produce the particleboards were obtained using volume fraction model [27]. Four particleboards were produced and investigated as shown in Figure 1f.

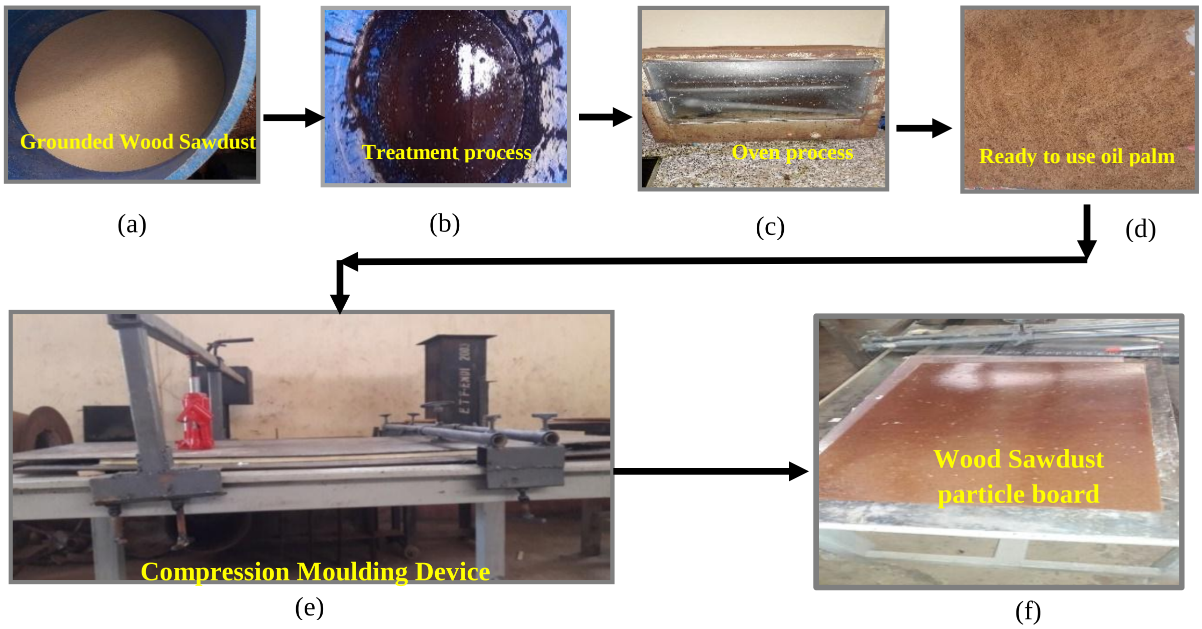

Figure 1: Fabrication process of the wood sawdust composite particleboard using hand Lay-up Compression Moulding

Table 1: Formulation of flame retardant loadings in the fabricated particleboard

Specimen I.D	WSP/Resin Ratio (wt.%)	% of FR Formulation*		
		ATH	APP/GAP (2:1)	CB
WSPP$_{0\%}$	20/80	-	-	-
WSPP$_{15\%ATH/CB}$	20/80	9	-	6
WSPP$_{15\%APP\text{-}GAP/CB}$	20/80	-	9	6
WSPP$_{18\%ATH/APP\text{-}GAP}$	20/80	9	6	3

Formulation of Flame Retardant specified in percentage relative to the total amount of resin

Table 1 illustrates the composition of the various WSPP produced as well as the required quantity of FR formulation added during fabrication. The required volume of PR obtained in a measuring cylinder was poured into a plastic container containing a measured FR percentage loading ratio which formed a paste solution. The paste was stirred thoroughly at room temperature and then the catalyst and accelerator was added for better interfacial adhesion. The paste was then cast into the mould as shown in Figure 1 and allow for a gel time of 5min before covering with an aluminium sheet. A 2-ton hydraulic press was used to apply pressure to the mould cover for dimensional stability. The particleboard was allowed 24hrs to cure at room temperature before demoulding and post cured for additional 3 days in air.

3.0 Characterization

3.1 Impact Test

Charpy impact test was performed on the fabricated composite particleboard using an impact tester in accordance with ASTM D 256 standards. From the particleboard the impact strength (IS) dimension (100x10x10mm) was obtained. Prior to mounting on the test machine, the test specimen was notched to a depth of 2mm with a v-shaped hand file. The notched test specimen was then mounted on the impact-testing machine, which is operated to impact a blow to fracture the specimen at the opposite end of the notch by releasing the suspended handle of the pendulum swing. The impact strength measured as the absorbed energy before fracture was then read off on the calibrated scale. The specimens were repeated three times and an average absorbed energy value recorded.

3.2 Flammability Properties

The cone calorimeter apparatus (CCA) was used to study the flammability properties of the fabricated wood sawdust particleboard according to ASTM E 1354. The specimens (100mm x 100mm x10mm) cut from the particleboard were wrapped in aluminium foil; along the side and bottom to reduce heat losses as specified in the standard. The specimens were exposed to $50kwm^{-2}$ heat flux horizontal orientation. During testing, the time to ignition (Tig), heat release rate (HRR), mass loss rate (MLR), residual mass and a sensible result was adopted for this study.

3.3 Flame Spread

Surface flame spread test were performed on the specimens according to ASTM E 1321 standard procedure using a radiant panel flame spread apparatus. The radiant heat energy panel is ignited using a propane flame and allowed to preheat for 30 min before commencing testing. A (500mm x 100mm x 10mm) specimen was slide between an aluminium frame with hinged front cover backed by a non-combustible board and a sample holder made of aluminium wire. Along the edge of the specimen holder there are every 25mm marks to aid in recording the flame spread rate. Video recordings of the moving flame front position were captured in real time surface for the flame front in order to derive the velocities. The position of the camera was perpendicular to the specimen burning surface to give a definite view of the flame front position as depicted in the experiment set-up in our previous research work [28]. The test was repeated three times for each specimen and average value recorded.

4.0 Particleboard Euro-classification by Convolution theorem

The predictive model used in calculating the particleboard heat release rate (HRR_{SBI}) in real-scale was derived from the works of Liu and Chen [29]. It is assumed that HRR in the SBI of the specimen at each location go through the same history as measured in the cone calorimeter. Hence, the HRR_{SBI} is then obtained using the convolution theorem known as Duhamel's integral as shown in [Eq. 1 and 2]. From the model predictions, the particleboards were classified according to Euro-classification systems [EN 13501-1:2002) [30]. The particleboard limitation to generation of spread of fire within buildings was predicted using standard equations; fire growth rate index (FIGRA) and total heat released [THR_{600s}].

$$\mathrm{HRR_{SBI}} = \int_0^{i} \dot{A}_{hrr,eff}(\tau)\dot{q}''_{cc}(t-\tau)d\tau \approx \sum_{I=1}^{N} \Delta A_{hrr,eff} \cdot \dot{q}''_{CC}{}^{N-1} \qquad [1]$$

Where,

$$A_{hrr,eff} = A_{max}\left[1 + \left(1 + \frac{t - \frac{t_{ig}}{2}}{t_{ig}}\right) exp\left(-\frac{t - \frac{t_{ig}}{2}}{t_{ig}}\right)\right] \qquad [2]$$

4.0 Results and Discussions

4.1 Impact Strength

In Figure 2, the results obtained for IS reveals that WSPP$_{15\%APP\text{-}GAP/CB}$ and WSPP$_{18\%ATH/APP\text{-}GAP/CB}$ particleboards maintained the same absorbed energy of 65.4 MPa with those without FR (WSPP$_{0\%}$). The FR acted as reinforcements which facilitated the stress transfer between the FR, WSP and PR as well as a close similarity of the WSP and the FR in shape could have enhanced the compactness of the WSPP. The decrease in IS affected by WSPP$_{15\%ATH/CB}$ from 65.4MPa to 58.8MPa (10% decrease) resulted from non-uniform dispersion coupled with agglomerated FR particles which provides locations of stress concentrations, thus provides sites for crack initiations. Besides ATH have been reported to increase in brittleness [31] which reduced the ability of composites to absorb and disperse energy. In this study, the addition of GAP played a significant role in enhancing the particleboard compactness and thus facilitated the transfer of stresses between the particles, PR and the FRs during blow.

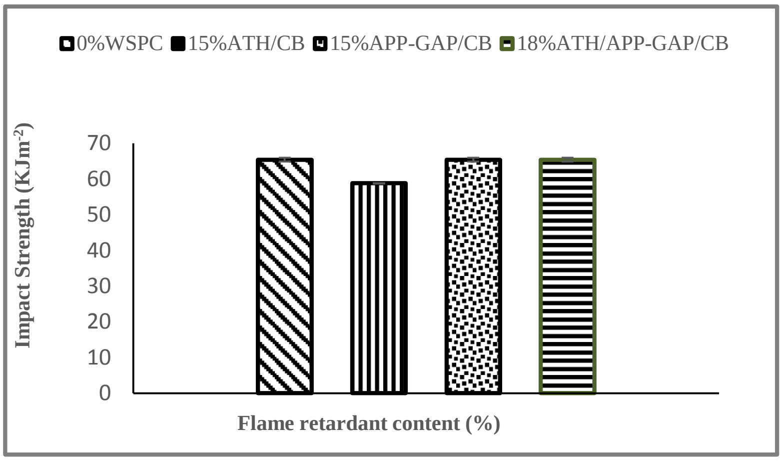

Figure 2: Impact strength data for WSP particleboard at varying flame retardant loadings

4.2 Flammability Properties

The fire risk of the particleboard was assessed through its time to ignition (Tig) response which quantifies the performance of a material in fire as well as its rapid flame spread. Table 2 reveals that the non-hybrid synergistic WSPP$_{15\%A\text{-}GAP/CB}$ and hybrid synergistic WSPP$_{18\%ATH/APP\text{-}GAP/CB}$ formulations observed in the cone calorimeter at 50kWm^{-2} significantly delayed Tig while the hybrid synergistic WSPP$_{18\%ATH/APP\text{-}GAP/CB}$ formulation could not delay longer the release of combustible volatiles. The particleboard with the highest delay in Tig contained the modified APP-GAP with CB that is WSPP$_{15\%APP\text{-}GAP/CB}$ formulation at 42s from 12s (250% decrease) compared to the WSCP$_{0\%}$. The mechanism of WSPP$_{15\%APP\text{-}GAP/CB}$ formulation which formed a stable compact char structure slowed the mobility of molecules in the polymer and prevented the release of combustible volatiles. It can further be elucidated that the presence of APP upon heating dehydrated the carbohydrate present in GAP to form stable char that prevented the release of combustible volatiles.

Table 2: Summary of flammability properties of the wood sawdust polyester panel

Specimen I.D	Tig (s)	HRRavg (kW/m^2)	HRR-peak (kW/m^2)	MLR-peak (gs-1m-^{2})	Rm (wt. %)
WSPP$_{0\%}$	12	109.6	195.5	0.306	7.3
WSPP$_{15\%ATH/CB}$	17	43.5	100	0.162	19.2
WSPP$_{15\%APP\text{-}GAP/CB}$	42	47.7	78	0.108	48.9
WSPP$_{18\%ATH/APP\text{-}GAP}$	46	32.8	56.1	0.213	43

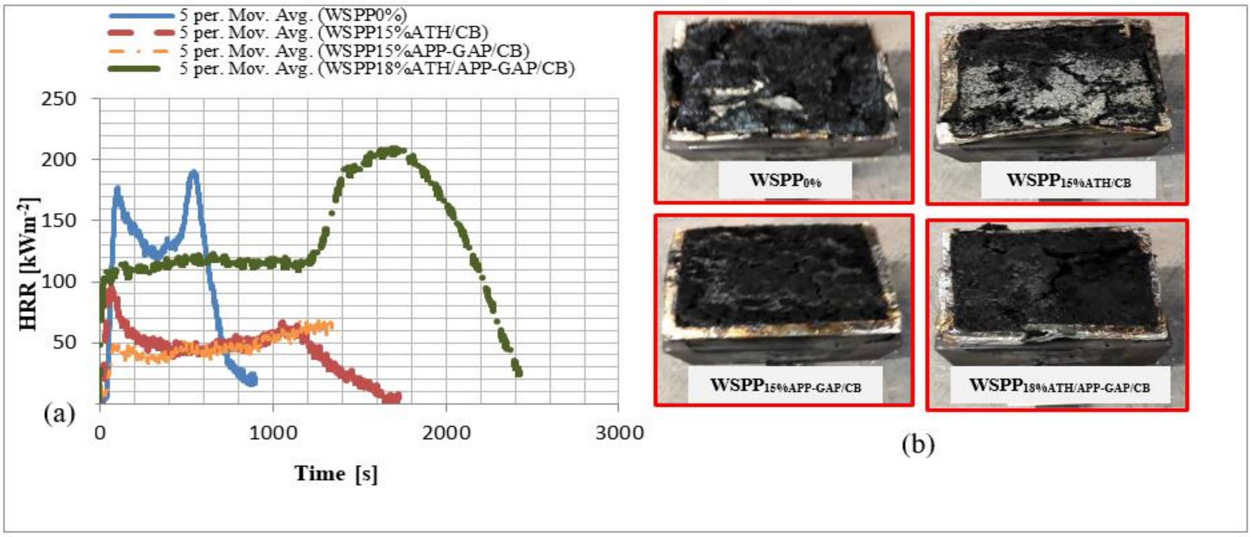

Figure 3: (a) Comparison of 0%WSPC panel heat release rate (HRR) curves with FR formulations (b) Char residue after cone calorimeter test at 50kW/m^2

The heat release rate (HRR) profile indicative of fire intensity and growth rate of the WSPP obtained from cone calorimeter is depicted in Fig. 3. The HRR is a key property in evaluating the particleboards limit to fire safety. From the HRR curves it is clearly seen that shortly after ignition, a sharp rise and then a sudden decline was observed for all the particleboard types which indicate the activities of the combustible products during combustion. It was observed that $WSPP_{0\%}$ and $WSPP_{18\%ATH/APP-GAP/CB}$ exhibited a double peak HRR, indicative of a failure in the char structure as reported by [Li et al [32]. When FRs were added to the particleboard it reveals a broader appearance which stayed at a lower profile throughout the burning process, indicative of the FR interaction with the combustible products. In table 2, it was found that the addition of the hybrid synergistic $WSPP_{15\%APP-GAP/CB}$ formulations in the particleboards exhibited an outstanding performance as the HRR-peak and HRR-avg indicating the intensity of fire and contribution to sustained fire respectively were remarkably reduced to 78kWm^{-2} from 195.5kWm^{-2} (60% decrease) and 47.7kWm^{-2} from 109.6kWm^{-2} (57% decrease) respectively compared to $WSPP_{0\%}$. The decrease could be elucidated by the effect APP-GAP with CB characteristic mechanism. APP-GAP inhibits the mass and volatile transfer between the condense phase and gas phase once a char layer is formed, thus it contributes to the reduction in HRR.

The MLR of the particleboard which is a measure of the dehydration reactions and pyrolysis was examined and presented as shown in Table 2. The MLR-peak (MLRp) of the hybrid synergistic $WSPP_{15\%APP-GAP/CB}$ particleboard was significantly reduced to 0.108gs^{-1} from 0.305gs^{-1} (65% decrease), indicative of slow decomposing particleboard compared to $WSPP_{0\%}$ which enhanced the residual mass (Rm) and suggest a good flame retardancy. Infact, the greater the decrease in MLR-peak the better the reduction in the HRRp was observed, this has also been confirmed by other authors [33-35]. The combustion residue displayed for the particleboards on the right hand side of Fig 3 after cone calorimeter test reveals that $WSPP_{0\%}$ displayed a loose and less dense char structure with exposed covering of aluminium foil which indicates more escape of combustible during the combustion process. In contrast, the hybrid synergistic $WSPP_{15\%APP-GAP/CB}$ left a mass of (48.9 wt. %) with black discontinuous dispersed like a toll structure and traces of white zone signifying intense combustion, slightly uniformly coherent which created a better barrier for the mass transfer of heat and attained the lowest HRRp of 78kWm^{-2}. This implies that both mass and heat transfer between condense phase and gas phase was restricted and consequently the underlying material protected from further combustion of the polymer pyrolysis. For the $WSPP_{15\%ATH/CB}$ particleboard it left a mass of white and black char structure with the appearance of cracks on the surface, this is similar to the $WSPP_{0\%}$. Notably, the $WSPP_{18\%ATH/APP-GAP/CB}$ particleboard exhibited visible cracks in the char structure of the underlying composite substrate indicating a high release of combustible products and the reason for the second HRR-peak.

5.3 Surface Flame Spread

The available energy (ϕ) in driving the flame to severe destruction is a measure of the heat transferred from the flame to the particleboard ahead of successive ignition. The estimate of the ϕ parameter as presented in Table 3 is a function of flame spread modulus, C and ignition parameter b obtained from the slope of the graphs as presented in (Appendix A1). The value of C was obtained by multiplying the slope of the graph by -√1000 to take care of the inconsistency in the units. The flame front velocity ($1/\sqrt{V_F}$) was calculated using the three-point least square fit to measure the flame front [36]. From the given table, it was observed that the non-hybrid synergist $WSPP_{15\%AH/CB}$ followed by the hybrid synergistic $WSPP_{15\%APP-GAP/CB}$ particleboards shows that the ϕ parameter was reduced significantly from 24.0 to 7.17KW^2s^{-3} (70.1% decrease) and 16.1KW^2s^{-3} (33% decrease) respectively relative to the $WSPP_{0\%}$. This is evident as ATH mechanism shows that ATH upon decomposition ATH releases water vapour which dilutes the combustible gases as well form aluminium oxide (Al_2O_3) which inhibited the forward heat transfer and thus weaken the flame energy leading to fire extinguishment. This can be further corroborated as the $WSPP_{15\%AH/CB}$ and $WSPP_{15\%APP-GAP/CB}$ particleboards travelled less distances of 65% each respectively compared to $WSPP_{0\%}$ particleboard which covered a distance of 80%. From the stages of the flame propagation as depicted in Fig 4b, it was observed that at the beginning of the test (i.e. at ignition and d=25mm) a steady, uniform, laminar flame was observed while as the burning proceeds somewhat to the middle (at d = 250mm), a turbulent behaviour was observed but began to recede early for $WSPP_{15\%AH/CB}$ and $WSPP_{15\%App-GAP/CB}$ particleboards compared to $WSPP_{0\%}$ indicative of a better interaction between the wood sawdust and FR.

Table 3: Flame spread parameters for the WSP particleboard

Specimen I.D	**b ($s^{-1/2}$)**	**C ($M^{3/2}kWs^{-1/2}$)**	**ϕ (kW^2s^{-3})**
$WSPP_{0\%}$	0.0282	8.17	24.0
$WSPP_{15\%ATH/CB}$	0.0337	12.5	7.17
$WSPP_{15\%APP-GAP/CB}$	0.0333	8.4	16.1
$WSPP_{18\%ATH/APP-GAP}$	0.0246	10.1	18.1

5.4 Particleboard Fire Behaviour by Classification

The profiles predicted by the model as displayed in (Appendix A2) is a series of predicted heat release rate (HRR_{SBI}) curves in the single burning item (SBI) compared to the cone calorimeter data which agrees with each other, especially in the early burning stage. The model predicts in full scale the fire behavior of materials during a fire scenario in this case the SBI as the fire reference scenario. The SBI test is a fire scenario use in classifying the contribution to fire of products and their related hazards. The model is a valuable tool for fire product development and quality control in relation to the new European classification for building products. The profile is seen to grow along the same paths with the measured profile in the cone calorimeter until it reaches its HRR-peak and then declined. The prediction of the first peak is usually adequate for predicting correctly the classification of the particleboards since the early part of the curve is of major importance in determining the fire growth rate (FIGRA) used in the Euro-classification. The main inputs parameters to the model are the time to ignition and heat release rate obtained in the cone calorimeter at 50kWm^{-2}. The effective heat release rate $A_{hrr,eff}$ in the SBI were obtained using standard procedure [28].

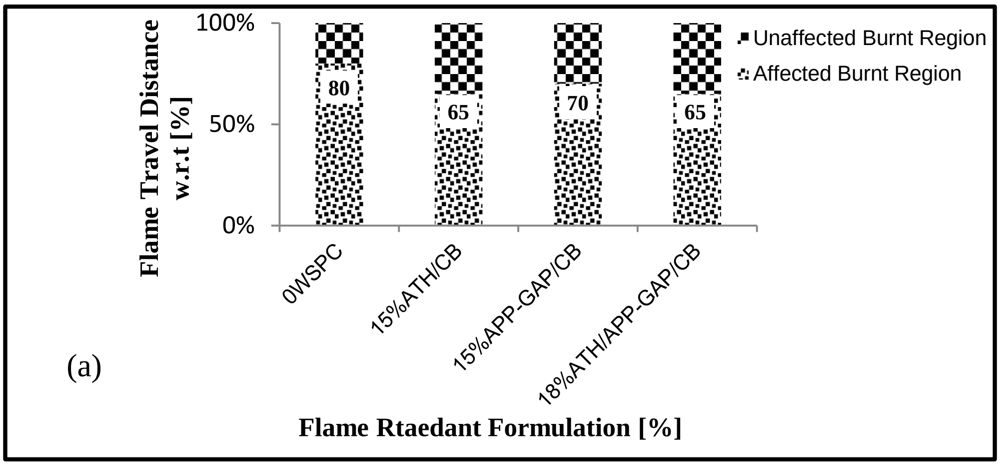

(b)

Figure 4: (a) Plots indicate visual measurement of the location of the pyrolysis front by observation. (b) Stages of flame front progression on the WSPP surfaces in real time.

Table 4: Predicted FIGRA values showing the level of fire hazards of WSPP

Specimen I.D	**FIGRA* [kW/s]**	**THR_{600} [MJ]**	**Euro-class**
$WSPP_{0\%}$	288	20.3	D
$WSPP_{15\%ATH/CB}$	174	3.3	C
$WSPP_{15\%APP\text{-}GAP/CB}$	57	2.8	B
$WSPP_{18\%ATH/APP\text{-}GAP}$	521	7.2	D

In calculating the parameters as input to the model, 30s sliding average was adopted as prescribed by the model description and this was carried out in excel Microsoft spreadsheet. In Table 4, the parameters used in classifying the hazards of the particleboards are presented. Based on FIGRA predictions, it was found that $WSPP_{0\%}$ reached a predicted FIGRA value of 388 kW/s. This placed the $WSPP_{0\%}$ in class (D) according to Euro-class criteria EN 13501-1 indicative of an acceptable contribution to fire which is similar to wood based products with thickness greater by 5mm tested in Euroclass [37]. With FR additions, the least FIGRA was observed for $WSCP_{15\%APP\text{-}GAP/CB}$ at 57kW/s which placed the particleboards in class B, indicative of very limited contribution to fire in real scale. The reason for the improved performance could be the high lignin content of the wood (20-30%) [38] and the mechanism of APP-GAP which formed compact char structure. APP upon heating releases phosphoric acid that dehydrates the (~97% carbohydrate) content in GAP [28] to form solid char structure and attained the highest residual mass as shown in Table 2.

Conclusions

In this paper, APP modified by GAP, hybridized with ATH and then synergized with CB in WSP particleboard was successfully achieved through hand lay-up compression moulding. Macro image observation shows that the modification of the hybrid system with GAP and CB improved the compatibility of the hybrid FR formulations to obtain optimum particleboard performance. Impact strength results show that hybrid synergistic $WSPP_{15\%APP\text{-}GAP/CB}$ and $WSPP_{18\%ATH/APP\text{-}GAP/CB}$ formulation maintained the same absorbed energy with $WSPP_{0\%}$ but decreased for the non-hybrid synergistic $WSPP_{15\%ATH/CB}$ because of the brittleness of ATH in composites. Cone calorimeter results show that the incorporation of $WSPP_{15\%APP\text{-}GAP/CB}$ in the WSP particleboard exhibited outstanding performance in flame retardancy as the Tig, HRR-peak, HRRavg, and MLR-peak improved significantly by 250%, 60%, 56%, and 65% respectively due to the decomposition mechanism of the of APP-GAP system which caused a stable compact char preventing the release of combustible volatiles. Studies of the char structure further reveals that a more stable and compact char structure formed protects the underlying particleboard substrate from combustion during the burning process. Radiant panel apparatus test shows that $WSPP_{15\%ATH/CB}$ and $WSPP_{15\%APP\text{-}GAP/CB}$ particleboards reduced the ϕ from 24.0 to 7.17KW^2s^{-3} and 16.1KW^2s^{-3} respectively and comparatively traveled less distances on the surface of the particleboard before extinguishment occurred due to the mechanism of ATH and APP-GAP. The FIGRA predictions for the particleboard show that $WSCP_{15\%APP\text{-}GAP/CB}$ exhibits a class B indicative of a limited contribution to fire in real scale and suitable to meet established fire safety standards in building applications.

Notations and Symbols

$\dot{A}$ = time derivative of the burning area

$A_{hrr,eff}$ = Effective heat release burning area

$t_{(s)}$ = time of ignition (s)

N = Total number of data recordings after ignition

$\dot{q}''_{cc}$ = HRR per unit area (N-i) time increments after ignition recorded in the cone calorimeter

ΔA = Incremental burning growth at time i

References

1. A.B. Akinyemi, J.O. Afolayan and E.O. Oluwatobi, Some Properties of Composite Corn Cob and Sawdust Particle Boards, *Construction and Building Materials*, 127 (2016) 436-441; https://doi.org/10.1016/j.conbuildmat.2016.10.040
2. Y.M.D. Adedeji, B. Ajayi Cost Effective Composite Building Panels for Walls and Ceilings in Nigeria in *11th Int. Inorganic-Bonded Fiber composite Conference* (2008)
3. P. Bazant, L. Munster, M. Machovsky, M. Sedlak J; Pastorek, Z. Kozakova, I. Kuritka, "Wood Flour Modified by Hierachical Ag/ZnO as Potential Filler for Wood Plastic Composites with Enhanced Surface Antibacterial Performance, *Ind. Crop Prod.* 62 (2014) 179-187; https://doi.org/10.1016/j.indcrop.2014.08.028
4. A. Ashori, Wood-plastic Composites as Promising Green-Composites for Automotive industries *Bio Resources Tecnol.* 99 (2008) 4661-4667
5. K.A. Afrifah, R.A Hickok and L.M. Matuana, Polybutene as a Matrix for Wood-Plastic Composites *Compos Sci Tenhol*, 70 (2010) 167-172
6. M.A. Binhussain and El-Tonsy Palm leave and Plastic Waste Composite for Out-Door Structure *Contr, Build Mater*, 47 (2013) 1431-1435
7. N. Ayrilmis, A, Kaymakci and T. Gulec, Potential use of Decayed Wood in Production of Wood Plastic Composite" *Ind Crop. Prod* 74 (2015) 279-284
8. A Schip and S. Su Effectiveness of Pre-Treated Wood Particles and Halogenated-Free Flame Retardants used in Wood-Plastic Composites, *Polym Degrad Stab* 126 (2016) 81-92
9. W Wang, S.F Zhang, F. Wang, Y.E Yan, J.Z Li, J.Z and W. Wang Effect of Microencapsulated Ammonium Polyphosphate on Flame Retardancy and Mechanical Properties of Wood-Flour/Polypropylene Composite" *Polym Compos*. 37 (2016) 666-673
10. N.M Stark, R.A White, S.W Mueller and T.A Osswald Evaluation of Various Fire Retardants for Use in Wood Flour-Polyethylene Composites, *Poly Degrad Stabil*. 95 (2010) 1903-1910

11. N.M Stark, R White, S.A Mueller and T.A Osswald, Effect of Fire Retardants on Heat Release Rate of Wood Flour-Polyethylene Composites *10th International Conference of Wood and BioFibre Plastic Composites,* (2009) p. 103-104
12. Z.X Zhang, J. Zhang, B.X Lu, Z.X Xin, C.K kan, J.K Kinn Effect of Flame Retardants on Mechanical properties, Flammability and Foamability of PP/Wood-Fiber Composite *Compos Part B*, 43 (2012) 150-158
13. C.E. Hobbs Recent Advances in Bio-Based Flame Retardant Additives for Synthetic Polymer Materials *Polymers* 11 (2019) 244 https://doi.org/10:390/polym11020224
14. Susan et al Halogenated Flame Retardants: Do the Fire Safety Benefits the Risk? *Review on Environmental Health,* 25 (4) (2019) 261-305 https://doi.org/10.1515/reveh.2010.25.4.261
15. J.Z Liang and Y.J Zhang A Study of the Flame Retardant Properties of Polypropylene/$Al(OH)_3$ /$Mg(OH)_2$ Composite" *Polym. Int*., 59 (2010) 539–542
16. W. Weng; Y Peng; M Zammarano and J. Li Effect of Ammonium Polyphosphate in Aluminium Hydroxide Mass Ratio on the Properties of Wood-Flour/Polypropylene Composites *Polymers,* 9 (2017) 615, doi:10.3390/polym9110615.
17. Z.B Shao, C. Deng, Y. Tan, L. Chen and Y,Z Wang Flame Retardation of Polypropylene via a Novel Intumescent Flame Retardant: Ethylene diamine-modified Ammonium Polyphosphate *Polym, Degrad Stab.* 106 (2014) 88-96
18. K. SLim, S.T Bee, L.T Sin, T.T Tee, C.T Ratman, D. Hui, A.R Rahmat A Review of Application of Ammonium Polyphosphate Intumescent Flame retardant in Thermoplastic Composites *Compos. Part B*, 84 (2016) 155-174
19. X.L Chen, Y.F Jiang and C.M Jiao Smoke Suppression Properties of Ferrite Yellow on Flame Retardant Thermoplastic Polyurethane Based on Ammonium Polyphosphate *J. Hazard Mater.* 266 (2014) 114-121
20. W Wang, Y. Peng, W. Zhang and J. Li Effect of Pentaerythritol of Wood-Flour/Polypropylene /Ammonium Polyphosphate Composite System *BioResources* 10 (4) (2015) 6917-6927
21. J.E Winandy State of the art paper: Effects of Fire-Retardant Treatments on Chemistry and Engineering Properties of Wood". *Wood Fiber Sci.* 45 (2013) 131–148
22. X.L Zhao, X.L.; Chen, C.K.; Chen, X.L. Effects of Carbon Fibers on the Flammability and Smoke Emission Characteristics of Halogen-Free Thermoplastic Polyurethane/Ammonium Polyphosphate, *J. Mater. Sci.* 51, 3 (2016) 762–3771
23. Y.L Ren, Y.L Wang, L.J Wang, T.T Liu Evaluation of Intumescent Fire Retardants and Synergistic Agents for use on Wood Four/Recycled Polypropylene Composites. *Constr. Build. Mater*, 76, 92015) p.273–278
24. W Wang, W Zhang, S.F Zhang, J.Z Li, Preparation and Characterization of Micro Encapsulated Ammonium Polyphosphate with UMF and its Application in WPCs. *Constr. Build. Mater*, 65 (2014) 151–158
25. W Wang Y. Peng, M. Zammarano, W. Zhang and J. Li Effect of Ammonium Phosphate to Aluminium Hydroxide Mass Ratio on the Properties of Wood-Flour/Polypropylene Composites *Polymers*, 9 (2017) 615-631.
26. P. Khalili, K.Y Tshai, and I. Kong, "Natural Fibre Reinforced Expandable Graphite Filled Composites: Evaluation of the Flame Retardancy, Thermal and Mechanical Performances *Composites Part A*, 100 (2017) 194 -205
27. https://sites.google.com/site/compositematerialsdesign/home/weight-and-volume-fractions
28. T.O Suoware, S.O Edelugo Thermal, Mechanical and Flame Spread properties of Oil Palm Fibre-Polyester panel" *SN Applied Sciences*. https://link.springer.com/article/10.1007/s42452-018-0048-1.
29. J Liu and M. Chen A Simplied Method to Predict the Heat Release Rate of Industrial Nitrocellulose Materials. *Applied Sciences* 8 (2018) 910; doi:10.3390/app8060910.
30. EN 13501-1 (2002) Fire Classification of Construction Products and Building Elements-Part 1: Classification using Test Data Form Reaction to Fire Test

31. A.M Redwen, K.H Badri and M.A Tarawneh The Effect of Aluminium Hydroxide (ATH) on Mechanical Properties and Fire Resistivity of Palm-Based Fibreboard prepared By pre-polymerization Method. *Advanced Materials Research* 1087 (2015) 287-292.
32. P Li, Y Zhang, Y Zuo, J Lu, G Yuan, Y Wu, Preparation and Characterization of Sodium Silicate Impregnated Chinese Fir Wood with High Strength, Water resistance, Flame Retardant and Smoke Suppression. *Journal of Materials Research and Technology* l 9(1) (2020) 1043-1053.
33. M. Nikolaeva and T. Karki Influence of Fire Retardants on the Reaction-to-Fire Properties of Coextruded Wood-Polypropylene Composites" Fire and Materials 40 (2016) 535-543
34. Y. Long, X. Zheng and Z. Jun Influence of Nanoparticle Geometry on the Thermal Stability and Flame Retardancy of High-Impact Polystyrene Nanocomposites *J. Thermal Anal Calorim*; 130 (2017) 1987-1996
35. W. Xin, W. Yujie G. Jiang, L. Jie, T. Nana, W Yanhui, J. Zhiwei, Q. Jian and T. Tao Thermal and Flammability Properties of Polypropylene/Carbon Black Nanocomposites *Polymer Degradation and Stability*, 97 (2012) 793-801
36. G Merryweather and M.J Spearpoint, M. J Flame Spread Measurement on Wood Products using the ASTM E 1321 LIFT Apparatus and a Reduced Scale Adaptation of the Cone Calorimeter *Fire and Materials*, 34(3) (2010) 109-136
37. T.D Hapuarachchi Development and Characterization of Flame Retardant Nano particulate Bio-based Polymer Composites" PhD thesis submitted to the University of London.(2010)
38. T.O Suoware, S.O Edelugo and I.C Ezema Flammability of Flame Retarded Natural Fibre Composites and Application in Automobile Interior: A Review" *imperial Journal of Interdisciplinary Research (IJIR)* 3, (8) (2017) 587-600

(2020) ; http://www.jmaterenvironsci.com

Appendix

A1: Graphs showing parameters used in obtaining flame spread modulus (C) and Ignition parameter (b)

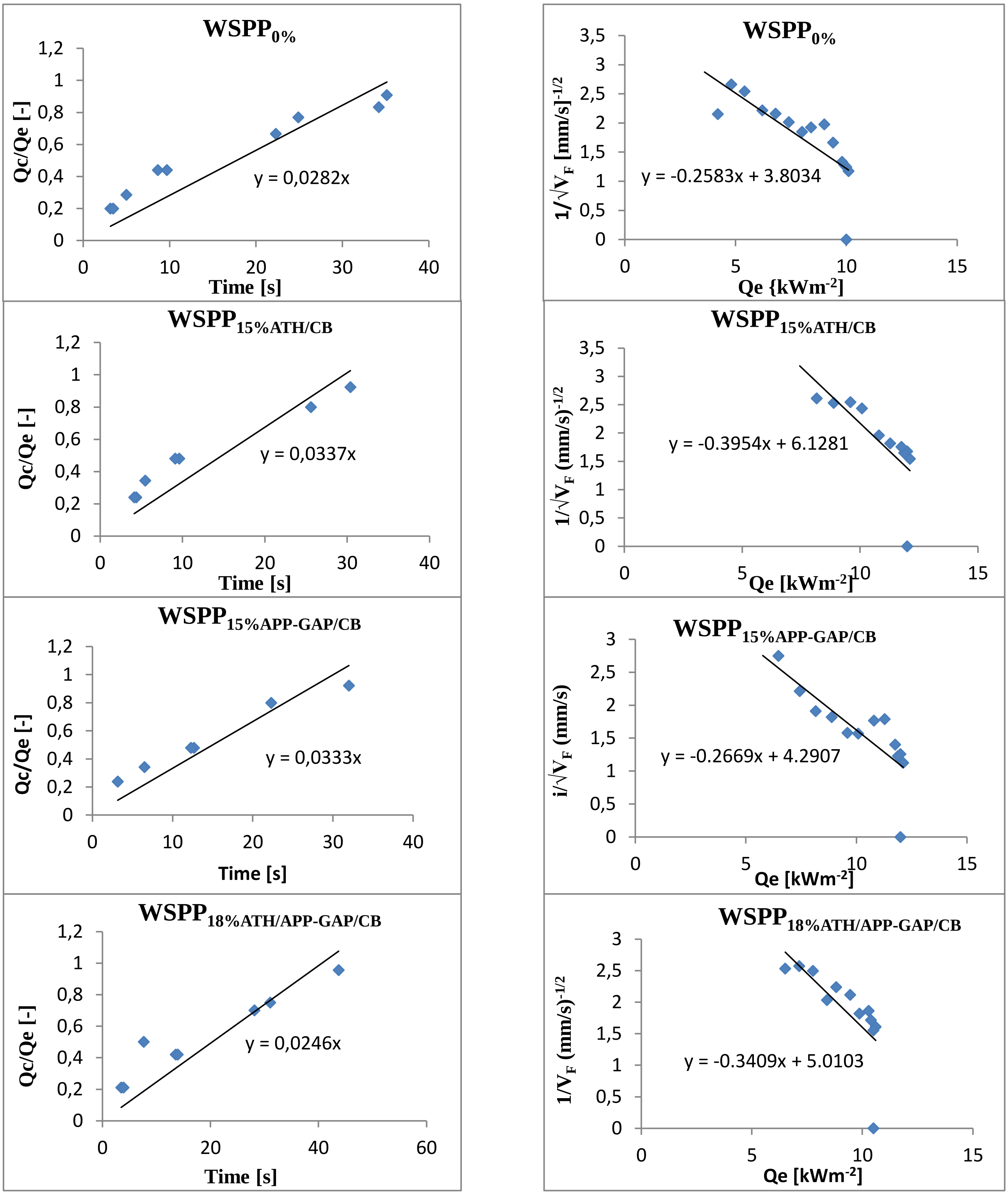

(2019) ; http://www.jmaterenvironsci.com

A2: Shows predicted curves of the WSC particleboard (a) HRR_{SBI} compared to HRR_{CC} data

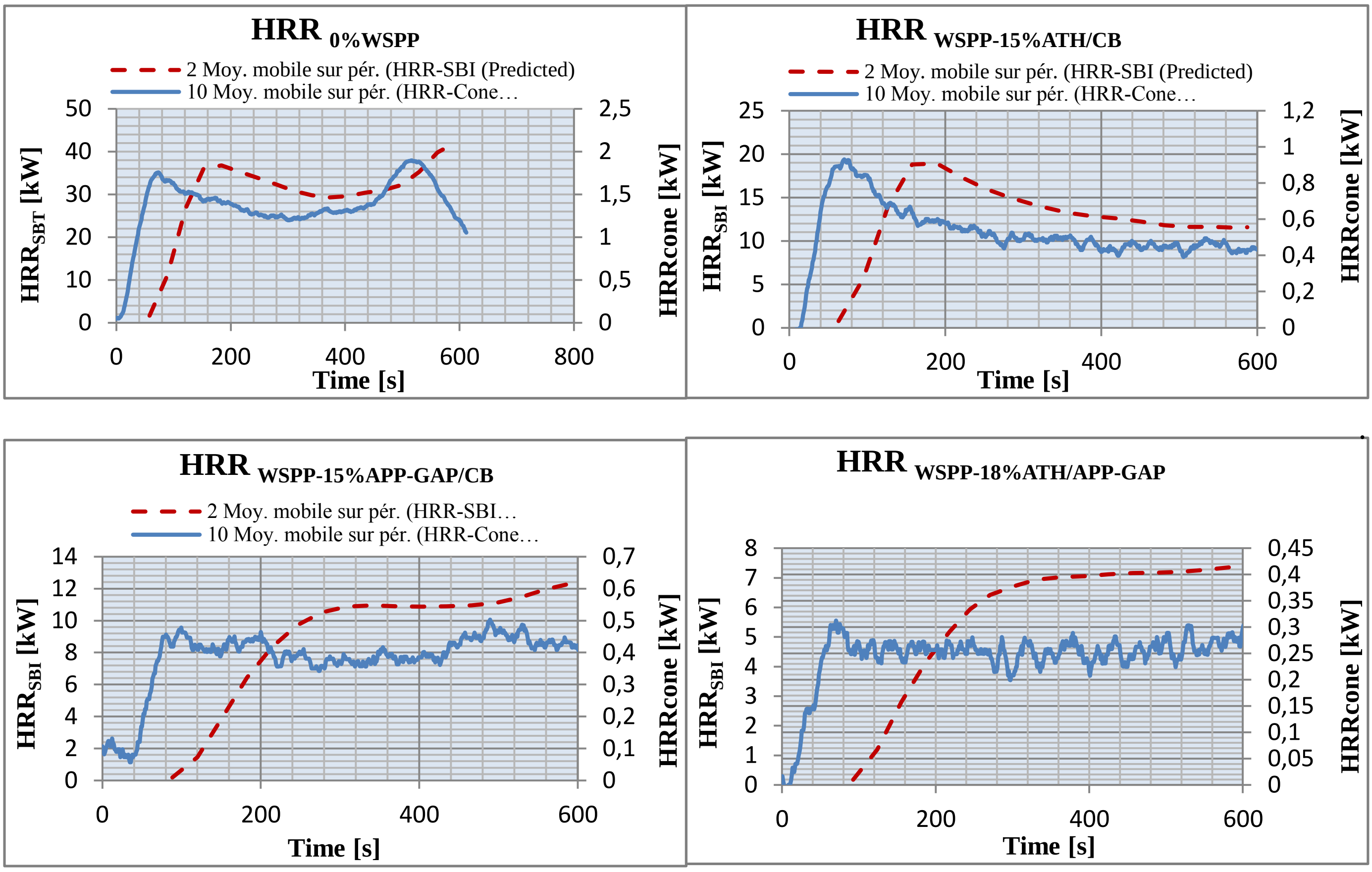

(2019) ; http://www.jmaterenvironsci.com